Special issue: the best paper of ENARC 2023

# Performance of Portland clinker produced through the incorporation of asbestos cement wast (ACW)

*Desempenho do clínquer Portland produzido através da incorporação de resíduo de cimento amianto (RCA)*

---

**Tiago Assunção Santos**
**Marcelo Strozi Cilla**
**Daniel Véras Ribeiro**

## Abstract

The production process of Portland cement has significant environmental impacts involving the exploitation of deposits for raw materials and $CO_2$ emissions. In this study, the incorporation of different proportions of asbesto cement waste (ACW) was evaluated, approximately 24%, 49%, 74%, and 86% by mass, corresponding to levels of 0.43%, 0.85%, 1.27%, and 1.69% of $SO_3$, respectively, replacing the limestone and clay mixture in Portland clinker blends. The effects of this incorporation on the clinkering process were analyzed at different temperatures (1300 °C to 1450 °C). The phases formed in the produced clinkers were identified through X-ray diffraction (XRD), followed by the grinding process for cement production, which was subsequently characterized physically. The hydration of pastes was monitored by XRD. Additionally, the mechanical performance of pastes made with the produced cements was also assessed. From the results obtained, it was observed that ACW acts as a mineralizer at lower clinkering temperatures (1350 °C), resulting in an increase in the alite ($C_3S$) content in the clinkers. Consequently, cements produced with ACW showed an increase in the amount of hydrated phases and superior mechanical strengths at early ages compared to the reference cement without the addition of ACW.

**Keywords:** Portland cement. Asbestos cement waste. Portland clinker. Paste hydration.

## Resumo

*O processo de produção do cimento Portland é responsável por elevados impactos ambientais. Neste estudo, foi avaliada a incorporação de diferentes proporções de RCA (aproximadamente 24%, 49%, 74% e 86% em massa, correspondendo a níveis de 0,43%, 0,85%, 1,27% e 1,69% de* $SO_3$*, respectivamente) em substituição à mistura de calcário e argila em blendas de clínquer Portland. Os efeitos dessa incorporação no processo de clinquerização foram analisados em diferentes temperaturas (1300 °C a 1450 °C). As fases formadas nos clínqueres produzidos foram identificadas por meio de difração de raios X (DRX), seguido pela produção dos cimentos, que foram posteriormente caracterizados fisicamente. A hidratação das pastas foi monitorada por DRX. Além disso, o desempenho mecânico das pastas confeccionadas com os cimentos produzidos também foi avaliado. A partir dos resultados obtidos, foi observado que o RCA atua como mineralizante em temperaturas mais baixas de clinquerização (1350 °C), resultando no aumento do teor de alita (*$C_3S$*) nos clínqueres. Como consequência, os cimentos produzidos com RCA apresentaram um aumento na quantidade de fases hidratadas e resistências mecânicas superiores em idades precoces quando comparados ao cimento sem adição de RCA.*

***Palavras-chave:*** *Cimento Portland. Resíduo de cimento amianto. Clínquer Portland. Hidratação das pastas.*

[1]**Tiago Assunção Santos**
[1]Universidade Estadual de Feira de Santana
Feira de Santana - BA - Brasil

[2]**Marcelo Strozi Cilla**
[2]Universidade Federal da Bahia
Salvador - BA - Brasil

[3]**Daniel Véras Ribeiro**
[3]Universidade Federal da Bahia
Salvador - BA - Brasil

**Recebido em 11/03/24**
**Aceito em 21/05/24**

SANTOS, T. S.; CILLA, M. S.; RIBEIRO, D. V. Performance of Portland clinker produced through the incorporation of asbestos cement wast (ACW). **Ambiente Construído**, Porto Alegre, v. 25, e139065, jan./dez. 2025.
ISSN 1678-8621 Associação Nacional de Tecnologia do Ambiente Construído.
http://dx.doi.org/10.1590/s1678-86212025000100818

# Introduction

Currently, there is significant emphasis on decarbonizing the built environment globally, considered a priority by the engineering community and related industrial sectors. One of the primary contributors to the global $CO_2$ emissions footprint in the built environment, and consequently a critical focus in efforts to achieve decarbonization, is the emission profile associated with construction materials during their production and use. The cement industry stands out as the major contributor, in terms of volume, to emissions related to construction materials. For this reason, it becomes a central focus in discussions on the need for decarbonization of the construction industry to minimize irreversible damage to the planet and its ecosystems.

In this context, the goal of achieving zero $CO_2$ emissions by 2050 assumes essential significance (IPCC, 2023). In 2020, cement production played a significant role in global human-caused $CO_2$ emissions, contributing approximately 7% to 8% of the total (CSI, 2021; WBCSD, 2012). Considering that approximately half of the cement produced worldwide is used in reinforced concrete structures (Cao *et al*., 2020), reducing the carbon footprint embedded in these structures emerges as a crucial strategy for the decarbonization process. This approach gains even more relevance in light of the projected annual increase of 2.2% in global demand for construction materials and infrastructure until 2060 (IRP, 2023).

A reduction in carbon dioxide emissions from combustion can be achieved by substituting fossil fuels with alternative fuels, optimizing the burners and calciners of the system, introducing new heating methods, or capturing carbon dioxide from the process. Additionally, the cement industry aims to replace limestone with secondary raw materials and calcium-rich waste from other industries, such as copper tailings (Ghazi; Jamshidi-Zanjani; Nejati, 2022), $TiO_2$ waste (Andrade Neto *et al*., 2022), granite rock fines (Gomes *et al.*, 2019; Santos *et al.*, 2022), eggshell waste (Her *et al*., 2022), and iron ore tailings (Young; Yang, 2019; Faria *et al*., 2023; He *et al.*, 2023).

In this scenario, the possibility of using Asbestos Cement Waste (ACW) in clinker production arises, whose chemical composition is similar to that of limestone and originates from fibrocement materials that have not been properly disposed of. With the identification of the carcinogenic potential of asbestos fibers (Stayner; Welch; Lemen, 2013), more than 75 countries have banned their exploitation, creating the need for alternatives to avoid improper disposal in landfills (Iwaszko; Zawada; Lubas, 2018). Spasiano and Pirozzi (2017) report that approximately 210 million tons of asbestos fibers were extracted worldwide between 1900 and 2015. According to Flanagan (2019), it is estimated that about 8.8 million tons of asbestos fibers were industrialized in Brazil between 1940 and 2018, resulting in over 100 million tons of asbestos tiles without proper disposal. Thus, the accumulated production of asbestos tiles in Brazil during this period was about 2.5 times the country's annual limestone production (approximately 40 million tons).

In a recent study, Santos, Cilla, and Ribeiro (2022) reported that the use of ACW in Portland clinker meal, replacing limestone, led to a reduction in $CO_2$ emissions by up to 11.85%. These authors also observed that the combined action of MgO and $SO_3$, present in ACW, accelerated the reactions in the clinkering process, increasing the percentage of $C_3S$ in the produced clinker. However, it is worth noting the scarcity of studies regarding the combined influence of these two oxides present in ACW on the polymorphism of $C_3S$ and $C_3A$.

Therefore, in this study, in addition to the mineralogical characterization of clinkers containing ACW, hydration analysis was conducted through X-ray diffraction (XRD). Finally, a physical-mechanical analysis of pastes produced with cements containing ACW was also performed.

# Materials and methods

## Materials

The ACW samples were taken from corrugated tiles collected from residences located in Salvador, Bahia, Brazil. These tiles were manufactured on a Hatscheck machine, with a nominal thickness of 4 mm, a width of 60 cm, and a length of 213 cm after approximately 23 years of exposure to weathering. This manipulation process was carried out in an isolated space and using equipment personal protective equipment such as gloves and masks. Figure 1 displays a micrograph captured by a TESCAN scanning electron microscope (SEM) at 15 kV (Vega 3 LMU model). The fractured section of a sample taken from the tiles reveals the presence of fibrous bundles, characteristic attributes of asbestos, similar to those described by Belardi and Piga (2013).

Table 1 presents the specific mass of particulate materials, determined using a helium gas pycnometer (AccuPyc II 1340 Micromeritics). Additionally, the specific BET surface area, obtained through a Gemini VII Micromeritics surface area analyzer, and the median equivalent diameters ($D_{50}$) obtained from the particle size distribution of the materials are provided. This distribution was analyzed using a laser diffraction particle size analyzer (CILAS 1180).

It is observed that the particles present in the ACW are finer compared to conventional raw materials. The presence of smaller particles in ACW in comparison to traditional raw materials such as clay and limestone may influence reactivity during the clinkering process.

As expected, limestone is predominantly composed of calcium oxide (Table 2), which is the main component of the raw mix. The clay used in the study showed high levels of silicon and aluminum oxides, which are the sources of these constituents in the meal. ACW exhibits a predominance of CaO (38.69%) and $SiO_2$ (13.16%), suggesting that this waste can serve as a partial substitute for limestone. Additionally, significant levels of MgO (6.97%) and $SO_3$ (1.69%) are found, data that align with previous studies conducted by Santos, Cilla, and Ribeiro (2022) and Ranaivomanana and Leklou (2021).

The mineralogical characterization of ACW (Figure 2) was conducted through X-ray diffraction using a Bruker X-ray diffractometer, model D2 Phaser (with a target tube: wavelength 0.154060 nm), set at 30 kV and 10 mA, without a secondary monochromator filtration system. Diffraction spectra were obtained for a scanning range (2θ) between 5° and 70°, with a continuous speed of 0.1°/s. The DifracEva software, incorporating the Crystallography Open Database (COD), was employed to identify the mineralogical phases.

Figure 1 – **Morphology of ACW after grinding, obtained by SEM**

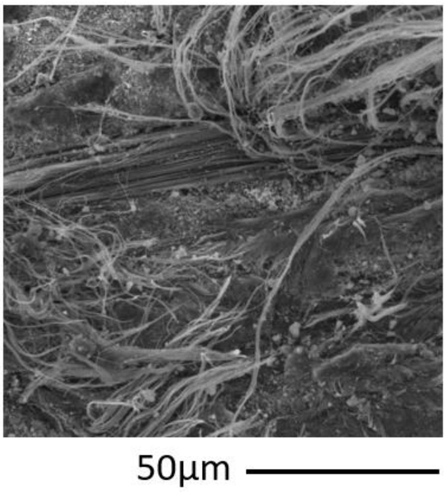

Table 1 – **Specific mass, $D_{50}$, and B.E.T specific surface area of limestone, clay, and ACW**

| Materials | Propriedades | | |
|---|---|---|---|
| | Specific mass ($cm^3/g$) | $D_{50}$ (μm) | Specific surface area B.E.T ($m^2/g$) |
| Limestone | 2.72 ± 0.13 | 2.40 | 12.26 ± 1.12 |
| Clay | 2.69 ± 0.52 | 7.14 | 6.17 ± 1.35 |
| ACW | 2.57 ± 0.10 | 1.80 | 30.38 ± 2.06 |

Table 2 – **Chemical composition of raw materials obtained by X-ray fluorescence**

| Materials | Contents (%) | | | | | | | | |
|---|---|---|---|---|---|---|---|---|---|
| | CaO | $SiO_2$ | $Al_2O_3$ | $Fe_2O_3$ | MgO | $K_2O$ | $SO_3$ | Other | LOI* |
| Limestone | 43.55 | 10.80 | 3.16 | 1.27 | 2.10 | 0.57 | -- | 0.18 | 38.20 |
| Clay | 0.24 | 58.29 | 23.50 | 4.77 | 1.18 | 1.38 | 0.12 | 1.10 | 8.47 |
| ACW | 38.69 | 13.16 | 2.4 | 2.42 | 6.97 | 0.35 | 1.69 | 0.63 | 33.65 |
| Gypsum | 32.14 | 2.07 | 1.00 | 0.25 | -- | 0.18 | 41.89 | 0.42 | 22.00 |

**Note**: *loss on igntion.

Figure 2 - **X-ray diffractogram of asbestos-cement tile waste, with identification of crystalline phases**

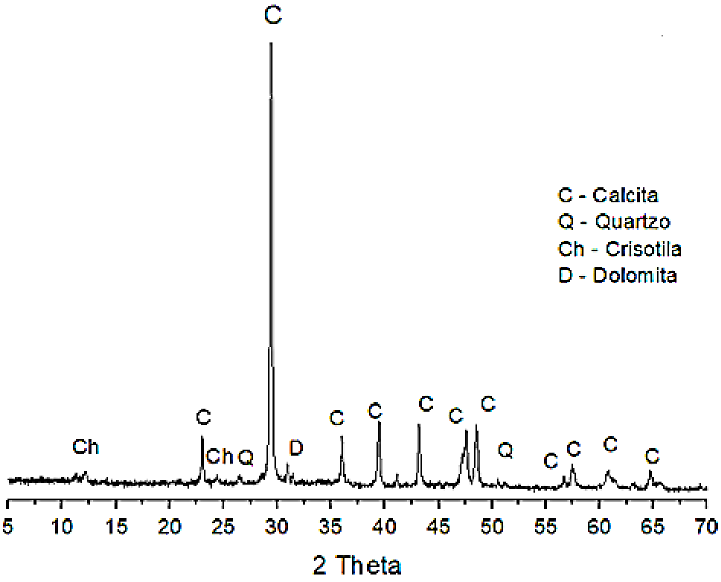

In the X-ray diffractogram of ACW, characteristic peaks of calcite ($CaCO_3$), quartz ($SiO_2$), chrysotile [$Mg_3Si_2O_5(OH)_4$], and dolomite [$CaMg(CO_3)_2$] were identified, minerals also identified by Viani and Gualtieri (2014) and Viani *et al.* (2013). However, these authors found other mineralogical phases in ACW, such as portlandite [$Ca(OH)_2$], belite β ($Ca_2SiO_4$), amphibole asbestos, and aragonite ($CaCO_3$), due to the variety of samples evaluated. In a recent study, Carneiro *et al.* (2021) reported that the presence of calcite and absence of hydrated compounds in ACW can also be justified by the carbonation of hydrated cement compounds, which typically occurs in a relatively short time due to the thin thickness of the tiles.

## Methods

### Clinker dosage and production

Table 3 presents the proportions of the raw mixes based on the various chemical compositions of the raw materials obtained by XRF. For the calculation of the raw mix, the values of LSF (Lime Saturation Factor) were kept at 98. The proportions of ACW, which replaced the combination of limestone + clay, were set at approximately 24.01%, 48.82%, 74.46%, and 85.76% by mass, resulting in a reduction in the limestone content by approximately 23.80%, 48.30%, 73.70%, and 84.90%, respectively, and in the clay content by approximately 28.00%, 57.00%, 86.80%, and 100.00%, respectively.

The LSF was set at 98 to ensure the formation of 70% alite in Portland clinker, as observed in previous studies conducted by Schoon *et al.* (2012), and Vilaplana *et al.* (2015). The chemical modules of the raw mix, as presented in Table 1, including the Silica Module (SM) and the Alumina Module (AM), were determined using Equations 1 to 3.

$$\mathrm{LSF} = \frac{100\mathrm{CaO}}{2.\mathrm{SiO_2}+1.2\mathrm{Al_2O_3}+0.65\mathrm{Fe_2O_3}} \quad \text{Eq. 1}$$

$$\mathrm{SM} = \frac{\mathrm{SiO_2}}{\mathrm{Al_2O_3}+\mathrm{Fe_2O_3}} \quad \text{Eq. 2}$$

$$\mathrm{AM} = \frac{\mathrm{Al_2O_3}}{\mathrm{Fe_2O_3}} \quad \text{Eq. 3}$$

According to the data presented in Table 1, it can be observed that clinkers produced with ACW exhibit contents of up to 4.35% by mass of MgO and 1.69% by mass of $SO_3$. Maki and Goto (1982) report that the presence of up to 1.80% of $SO_3$ can have a mineralizing effect on the clinkering process, as well as assisting in the burning of raw mixes. However, an excess of $SO_3$ in these mixes can result in a reduction in the $C_3S$ content formed, leading to higher emissions of $SO_2$ gases and corrosion in rotary kilns (Taylor, 1997). Thus, the incorporation of $SO_3$ should be limited to 2% by mass (Chatterjee, 2011).

Table 3 – **Design of the mix, chemical modules, and expected levels of $SO_3$, MgO, and equivalent alkalis in clinkers produced from the incorporation of ACW**

| Raw mix | Proportion in Materials (%m) | | | Chemical parameters | | | Expected content (%m) | | |
|---|---|---|---|---|---|---|---|---|---|
| | Limestone | Clay | ACW | LSF | AM | SM | $SO_3$ | MgO | Eq* |
| CL-AC0 | 95.29 | 4.70 | 0.00 | 98 | 2.88 | 2.35 | 0.01 | 2.02 | 0.40 |
| CL-AC24 | 72.05 (-23.8%) | 3.94 (-28.0%) | 24.01 | 98 | 2.22 | 2.41 | 0.43 | 2.61 | 0.45 |
| CL-AC49 | 48.82 (-48.3%) | 2.36 (-57.0%) | 48.82 | 98 | 1.72 | 2.51 | 0.85 | 3.19 | 0.49 |
| CL-AC74 | 24.82 (-73.7%) | 0.72 (-86.8%) | 74.46 | 98 | 1.29 | 2.63 | 1.27 | 3.77 | 0.54 |
| CL-AC86 | 14.24 (-84.9%) | 0.00 (-100%) | 85.76 | 98 | 1.12 | 2.69 | 1.69 | 4.35 | 0.59 |

**Note**: *equivalent alkalis.

It was also observed, in some raw mixes with ACW, that the MgO contents (4.35%) are lower than the permissible normative value for Portland cements (6.50%), stipulated by NBR 16697 (ABNT, 2018). This phenomenon indicates that such raw mixes may not produce cements with MgO contents higher than required by the standard. Finally, it is noted that the content of equivalent alkalis ($Na_2O + 0.658 \cdot K_2O$) in the raw mixes with ACW ranges from 0.40% to 0.59%.

After the dosing of the raw materials, homogenization was carried out in the horizontal rotary mill QUIMIS, model Q298. The clinker production process followed the methodology adopted in the studies by Gomes *et al.* (2019), simulating the industrial stages of raw material homogenization and pre-calcination, as well as clinker sintering and cooling for laboratory production.

For the manufacture of the clinkers, pellets of the raw material were prepared with an approximate mass of 1.50 g and a diameter of 1 cm. To make these pellets, a water content of 20% (by mass) was added to provide workability to the material and achieve the appropriate consistency. The pellets were dried in an oven at 100 °C for 12 hours and then placed in alumina crucibles. Subsequently, they were sintered in a Nabertherm furnace (model LHT 02/17 LB Speed) with a heating rate of 5 °C/min until reaching 900 °C, remaining at this temperature for 30 minutes. In the second heating stage of the pellets, the same heating rate (5 °C/min) was used until reaching the final temperature (1300 °C, 1350 °C, 1400 °C, and 1450 °C), where they remained for 15 minutes before being rapidly cooled (190 °C/min) for the production of experimental clinkers.

## Mineralogical characterization of clinkers

In order to analyze the phases present in the produced clinkers, X-ray diffraction (XRD) technique was employed. Diffraction spectra were acquired in the range of 10° to 70° (2θ), using a continuous mode at a rate of 0.1°/s. The same equipment and configurations described in section 2.1 were used for this analysis.

Table 4 presents a summarized overview of the main information regarding the clinker phases and their respective ICSD cards, which were used in the quantitative evaluation conducted through the Rietveld method.

## Production and characterization of Portland cement

For cement production, 6.00% of gypsum was added to the clinker by mass, and then the samples were homogenized in a vertical rotary mill with steel balls, a Union Process Szegvari Attritor model, rotating at 700 rpm for 2 hours. According to the chemical analysis of the gypsum, it is possible to estimate, according to calculations suggested by C 150 (ASTM, 1997), that the added $SO_3$ content in the cement manufacturing was 2.50%. Thus, it is noted that the amount of sulfur trioxide (mass%) added is less than or equal to 4.50% for all types of cement (ABNT, 2018). Subsequently, the cements underwent characterization, including the determination of specific mass (by helium gas pycnometry), specific surface area by the Blaine method (using the automatic permeameter BSA 1 ACMEL), B.E.T. surface area, and particle size distribution (using the CILAS particle analyzer, model 1180).

Table 4 – **Mineralogical phases of Portland clinker, along with the ISCD code of the crystallographic cards used in X-ray diffraction (XRD) analyses**

| Mineralogical phases | ISCD CODE | Reference |
|---|---|---|
| $C_3S$ | 162744 | De la Torre *et al.* (2007) |
| $C_3A$ | 1841 | Mondal and Jefferey (1975) |
| $C_4AF$ | 9197 | Colville and Geller (1971) |
| Periclase | 9863 | Sasaki, Fujino and Takéuchi (1979) |
| Free lime | 28905 | Primak, Kaufman and Ward (1948) |

### Production and characterization of cement pastes

For the cement paste molding, a mixer with a speed of 300 rpm in a plastic container was used for a period of 1 minute, with a water-to-cement ratio of 0.4, without the addition of chemical additives. The decision was made to use small-sized cubic specimens due to the scarcity of material produced on a laboratory scale, which makes it impractical to manufacture the cylindrical specimens recommended by NBR 7215 (ABNT, 1996). This standard establishes the fabrication of cylindrical mortar specimens, with a diameter of 50 mm and a length of 100 mm, requiring a larger amount of cement. Demolding was performed after 24 hours, and the specimens were cured by immersion in water at room temperature (25.0 ± 2.0 °C). Subsequently, XRD analysis and compressive strength tests were conducted.

### Analysis of the hydration process

The evolution of the cement hydration process in cement pastes was monitored through X-ray diffraction at the ages of 1, 3, 7, 28, and 91 days. Diffraction spectra were obtained in the range of 5° to 60° (2θ), using a continuous mode at 0.1°/s. For this purpose, at the mentioned ages, the pastes were placed and kept in an oven at 40 °C for about 5 hours to eliminate free water and allow grinding. This temperature was chosen because above 45 °C, thermal decomposition of C-S-H and ettringite occurs. The hydration process of these cements was also evaluated by X-ray diffraction, using the same equipment and parameters detailed in the mineralogical analysis of the clinkers.

### Mechanical strength of cement

The mechanical compressive strength was determined using the method proposed by Mehta and Gjorv (1974) and adopted by Costa (2013), which utilizes specimens on a reduced scale, requiring a smaller amount of cement. Compressive strengths of paste specimens, produced with experimentally obtained cements, were verified using cubic specimens of approximately 15 x 15 x 15 $mm^3$ (Figure 38). Tests were conducted on an INSTRON 23-10 universal testing machine, equipped with a 10 kN load cell, with displacement control and a loading rate of 0.2 $N/mm^2$.

The results of mechanical strength will also include ANOVA statistical analyses of the produced cement samples. Assessments of significance and model lack of fit are obtained through analysis of variance (ANOVA), with a significance level of 95% ($\alpha = 0.05$).

### Expansibility

For the expansion test, Le Chatelier needles were used as proposed by the Brazilian standard NBR 11582 (ABNT, 1991), similar to BS EN 196-3 (BSI, 2005). After preparing the pastes, it was possible to obtain cold strength, which is expressed by the difference in distance between the needles over seven days immersed in potable water at a temperature of 23 °C. Cold expansibility allowed for analyzing the influence of MgO on the cementitious matrix.

# Results and discussion

## Mineralogical characterization of clinkers

In Figures 3 to 6, X-ray diffraction (XRD) spectra of reference clinkers (CL-0) and clinkers containing 24%, 49%, 74%, and 86% of ACW produced at temperatures of 1300 °C (Figure 3), 1350 °C (Figure 4), 1400 °C (Figure 5), and 1450 °C (Figure 6) are presented.

Figure 3 **- X-ray diffractograms of clinkers produced with 24%, 49%, 74%, and 86% ACW content replacing the limestone + clay mixture, at 1300 °C**

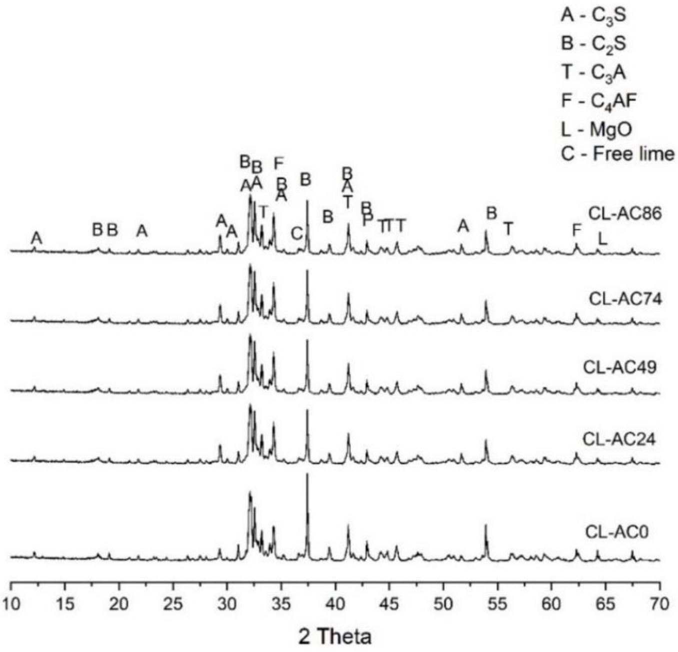

Figure 4 **– X-ray diffractograms of clinkers produced with 24%, 49%, 74%, and 86% ACW content replacing the limestone + clay mixture, at 1350 °C**

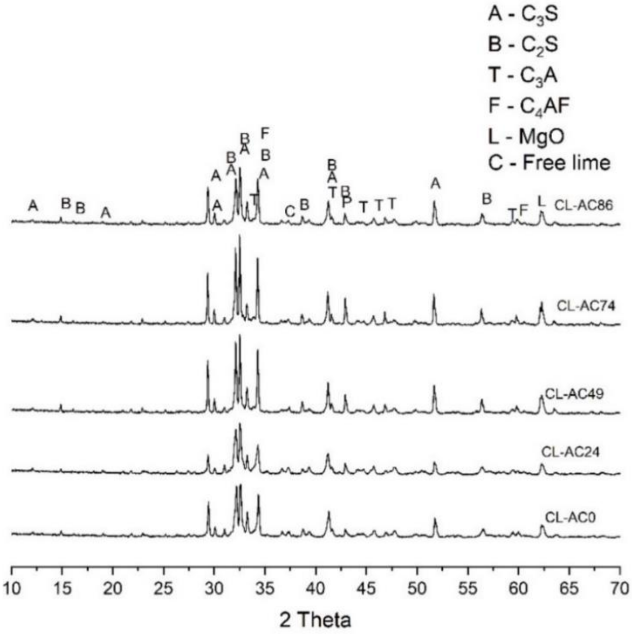

Figure 5 - **X-ray diffractograms of clinkers produced with 24%, 49%, 74%, and 86% ACW content replacing the limestone + clay mixture, at 1400 °C**

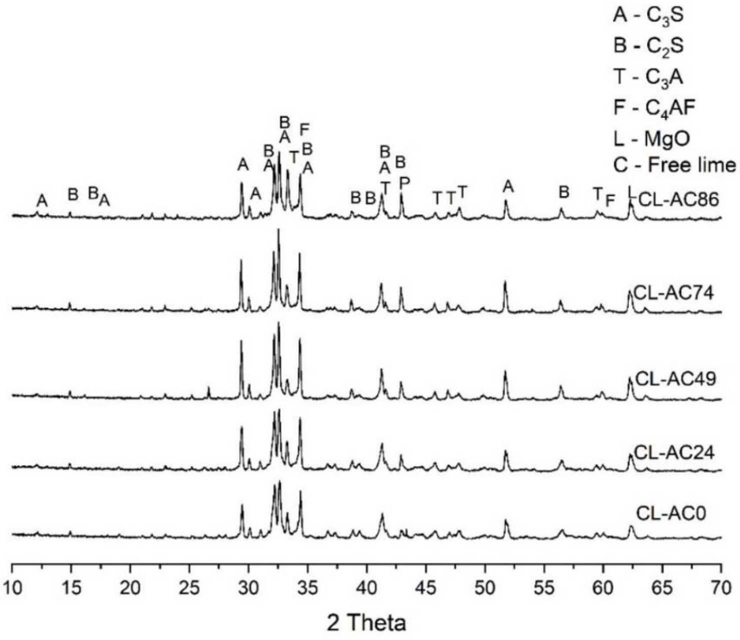

Figure 6 - **X-ray diffractograms of clinkers produced with 24%, 49%, 74%, and 86% ACW content replacing the limestone + clay mixture, at 1450 °C**

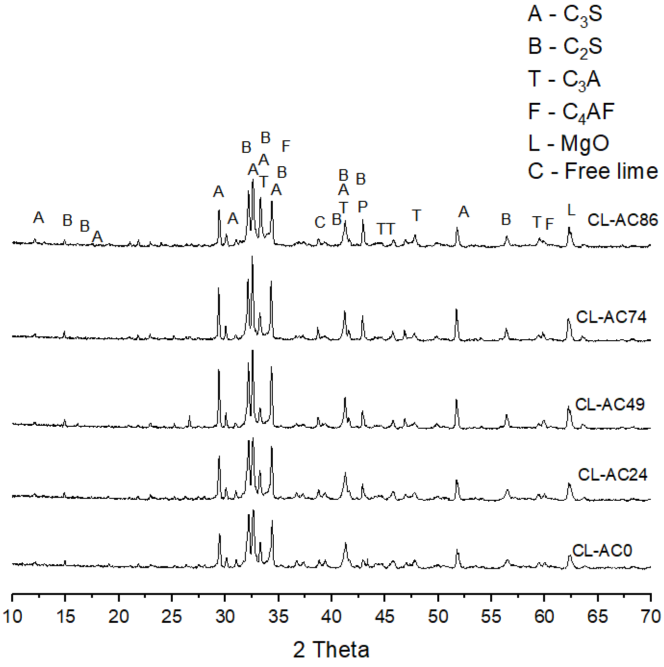

From the X-ray diffraction patterns shown in the aforementioned figures, peaks related to the main crystalline phases of Portland clinker (alite, belite, tricalcium aluminate, and tetracalcium aluminoferrite) are observed. Additionally, the absence of the chrysotile mineral phase, commonly found in asbestos tiles, is noteworthy. Santos, Cilla, and Ribeiro (2022) report that this phenomenon can be explained by the dehydroxylation of the fibers and the breakdown of amorphous anhydrides.

Table 5 presents the results of the quantitative analysis obtained through the Rietveld method. Although the produced clinkers have considerable alkali and $SO_3$ contents in their chemical composition, it was not possible to identify the presence of alkali sulfates, such as aphtitalite, ca-langbeinite, and arcanite, through XRD analysis. It was also observed that the presence of ACW did not lead to the formation of any additional phases, which is consistent with studies conducted by Schoon *et al.* (2012), who also evaluated the use of this waste in Portland clinker production.

Based on the results presented in Table 5, it can be noted that clinkers obtained at temperatures of 1350 °C, 1400 °C, and 1450 °C, containing a proportion of up to 86% of ACW with 1.69% of $SO_3$, showed higher amounts of alite ($C_3S$) compared to the reference clinker (without ACW). The most promising results were achieved with an addition of 74% of ACW, resulting in approximately 1.27% of $SO_3$.

Taylor (1997), Sohn *et al.* (2012), Schepper *et al.* (2013), and Boháč *et al.* (2022) report that the addition of $SO_3$ (up to 1.0%) to the raw mix reduces the formation temperature and viscosity of the liquid phase, increasing the diffusion of calcium ions, and consequently, the alite content at low temperatures. Additionally, the MgO present in Portland clinker raw mixes (up to approximately 4.35%) can also reduce the viscosity of the liquid phase formed during the clinkering process, facilitating the diffusion of calcium ions towards $C_2S$ crystals and reducing the Ca/Si ratio, accelerating the formation of alite in the clinker (Kolovos *et al*., 2001; Maki *et al*., 1993; De La Torre *et al.*, 2007).

Kolovos *et al.* (2001) and Yang *et al.* (2023) investigated the effects of minor elements present in the raw mix in the $CaO–SiO_2–Al_2O_3–Fe_2O_3$ system, observing that compounds containing $SO_3$ enhance the reactivity of the mixture, accelerating the combination of CaO, especially during the final stage of clinkering. In another study conducted by Raina and Janakiraman (1998), it was concluded that the presence of $SO_3$ accelerates the decomposition of $CaCO_3$ at lower temperatures, resulting in reduced energy consumption. Moreover, the presence of this oxide favors the growth of $C_3S$ crystals, facilitated by the formation of the liquid phase at lower temperatures. However, Katyal *et al.* (1998) emphasize that high concentrations of $SO_3$, above 2.50%, have a significant negative impact on the formation of $C_3S$ crystals during clinker production.

In clinkers subjected to calcination at 1300 °C, a lower alite content below the acceptable standard was observed. This content was even lower in clinkers containing ACW, suggesting that the temperature used was insufficient for the proper development of $C_3S$ crystals.

Table 5 - **Mineralogical compositions (%) of reference clinkers (CL-AC0) and those with the addition of different levels of ACW in substitution for the clay + limestone mixture, produced at temperatures of 1300 ˚C, 1350 ˚C, 1400 ˚C, and 1450 ˚C, obtained by the Rietveld method**

| **Mixes** | | **Content (%)** | | | | | | **Indicators** | |
|---|---|---|---|---|---|---|---|---|---|
| | | **$C_3S$** | **$\beta C_2S$** | **$C_3A$** | **$C_4AF$** | **f-MgO** | **f-CaO** | **$R_{wp}$*** | **GOF**** |
| 1300 °C | CL-AC0-1300 | 45.60±2.10 | 40.00±2.00 | 8.20±0.60 | 1.90±0.80 | 1.8±1.50 | 2.60±1.50 | 11.30±1.80 | 1.30±0.10 |
| | CL-AC24-1300 | 26.10±0.60 | 60.60±0.60 | 7.90±0.30 | 2.10±1.50 | 1.3±0.50 | 0.10±0.10 | 12.70±0.70 | 2.90±0.70 |
| | CL-AC49-1300 | 22.90±0.70 | 56.00±1.00 | 8.00±0.30 | 2.20±0.50 | 9.6±0.74 | 1.40±0.50 | 14.70±0.80 | 3.30±1.40 |
| | CL-AC74-1300 | 22.50±1.50 | 60.00±1.00 | 7.30±1.10 | 4.10±0.30 | 6.0±1.23 | 0.20±0.00 | 11.00±1.20 | 1.80±0.70 |
| | CL-AC86-1300 | 13.90±2.20 | 65.00±2.00 | 7.90±0.90 | 3.00±0.20 | 9.8±1.89 | 0.50±0.20 | 10.00±0.30 | 3.40±0.70 |
| 1350 °C | CL-AC0-1350 | 46.40±6.20 | 33.20±1.30 | 9.80±0.10 | 2.40±0.80 | 8.0±2.50 | 0.40±0.30 | 13.00±0.40 | 2.80±1.70 |
| | CL-AC24-1350 | 58.20±5.10 | 21.60±4.00 | 7.50±0.10 | 2.80±0.50 | 10.0±1.20 | 0.00±0.00 | 13.50±3.10 | 3.80±0.30 |
| | CL-AC49-1350 | 63.20±0.40 | 18.00±1.90 | 9.50±0.90 | 3.40±1.60 | 5.50±1.10 | 0.50±0.10 | 11.30±1.40 | 4.00±0.70 |
| | CL-AC74-1350 | 64.90±1.20 | 16.20±2.00 | 7.40±0.30 | 3.80±0.80 | 7.80±1.45 | 0.00±0.00 | 9.80±2.40 | 3.20±0.70 |
| | CL-AC86-1350 | 57.40±0.50 | 17.20±2.70 | 8.1±1.500 | 3.80±0.70 | 13.30±1.53 | 0.30±0.10 | 11.80±2.50 | 4.30±2.50 |
| 1400 °C | CL-AC0-1400 | 55.60±2.10 | 26.90±1.80 | 9.5±0.500 | 3.60±0.90 | 4.40±0.90 | 0.40±0.00 | 10.70±0.70 | 2.30±0.70 |
| | CL-AC24-1400 | 57.00±2.70 | 23.01±0.75 | 8.60±1.20 | 1.60±1.30 | 9.80±2.69 | 0.00±0.00 | 10.90±1.00 | 4.50±1.00 |
| | CL-AC49-1400 | 61.70±2.90 | 22.80±2.90 | 8.70±0.20 | 2.90±1.70 | 4.00±4.80 | 0.00±0.00 | 9.40±0.70 | 3.10±0.70 |
| | CL-AC74-1400 | 62.90±0.60 | 21.80±0.30 | 8.80±0.20 | 3.30±0.80 | 3.30±3.50 | 0.00±0.00 | 8.30±0.60 | 2.90±0.60 |
| | CL-AC86-1400 | 57.50±2.40 | 19.10±1.10 | 9.10±0.50 | 2.80±0.70 | 11.60±1.89 | 0.00±0.00 | 11.10±0.70 | 2.80±0.70 |
| 1450 °C | CL-AC0-1450 | 54.10±0.20 | 31.30±0.30 | 8.70±1.45 | 3.80±0.70 | 2.10±1.23 | 0.00±0.00 | 10.40±1.90 | 1.60±1.80 |
| | CL-AC24-1450 | 55.30±3.30 | 24.70±0.60 | 6.60±0.90 | 3.30±0.20 | 10.20±1.45 | 0.00±0.00 | 13.50±0.90 | 3.00±0.90 |
| | CL-AC49-1450 | 60.80±0.30 | 20.30±1.70 | 6.30±1.30 | 5.50±0.20 | 7.10±2.50 | 0.00±0.00 | 12.80±2.10 | 2.90±2.10 |
| | CL-AC74-1450 | 62.70±0.20 | 15.80±0.70 | 6.70±1.30 | 3.80±1.30 | 11.10±2.40 | 0.00±0.00 | 13.00±0.80 | 2.10±0.80 |
| | CL-AC86-1450 | 56.80±3.20 | 17.00±1.10 | 7.00±0.80 | 7.10±3.00 | 12.20±3.50 | 0.00±0.00 | 13.40±0.50 | 4.00±0.50 |

**Note**: *Quality of the Rietveld analysis fit, which should be below 5.**weighted profile factor indicating the quality of quantitative analysis, which should be below 15.

Regarding the formation of aluminates, a small reduction in the $C_3A$ content can be observed with the increase in the addition of ACW in the raw mix. This phenomenon can be explained by the fact that ACW has a lower aluminum content compared to the content present in clay. Thus, by replacing part of the clay and limestone mixture with ACW, there is an increase in the silica module (see Table 1), resulting in higher silicate content at the expense of aluminates (Winter, 2012). According to the XRD analysis of the clinkers, the undesirable presence of periclase (f-MgO) was observed, which, when in excess, can result in expansive reactions in the cement. The levels found in various experimental clinkers (up to 13.3%) exceed the permissible normative value (6.50%), indicating that the clinkers may present expansibility issues due to the presence of periclase. The free lime content in the clinkers calcined at 1350 °C, 1400 °C, and 1450 °C was below 0.5%, indicating an effective clinkering process. In some clinkers calcined at 1300 °C, a small increase in free lime content was noticed, indicating that this temperature is not sufficient for the production of Portland clinkers.

Finally, based on these analyses, it was observed that the clinkers with the addition of 49% and 74% ACW obtained at 1350 °C showed similar alite contents to those produced at 1400 °C. Therefore, aiming to produce cements at lower temperatures with lower environmental impact, it was decided to use clinker for the production of cements without and with the addition of 49% and 74% ACW at 1350 °C, in addition to the temperature commonly used in the industry (1450 °C), for comparative analysis.

## Cement characterization

### Physical characterization

Figure 7 illustrates the particle size distribution of the laboratory-scale produced cements with and without the incorporation of ACW. The analysis of the particle size distribution revealed similarities between the experimental cements with ACW after mechanical treatment, highlighting very close D50 values. Table 6 shows the values of D10, D50 and D90 of cements.

Figure 7 – **Particle size distribution of the reference cement (CEM-AC0) and with the addition of 49% and 74% ACW replacing the clay + limestone mixture, produced at temperatures of 1350°C and 1450 °C**

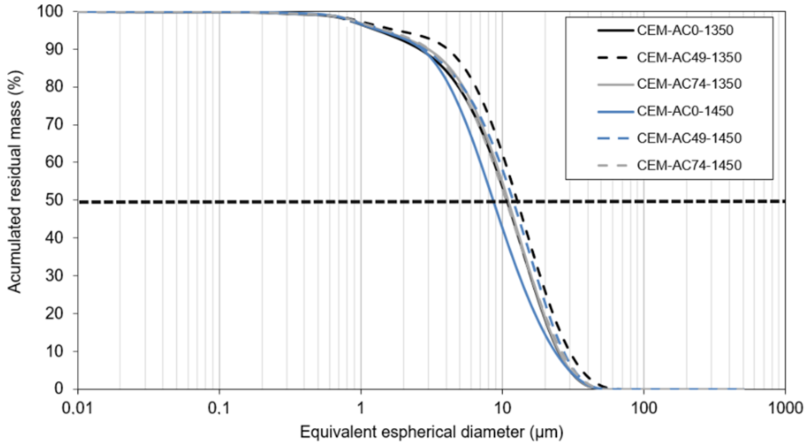

Table 6 – **Specific mass, surface area (Blaine and B.E.T), and loss on ignition (LOI) of reference cements (CEM-AC0) and with the addition of 49% and 74% ACW in substitution for the clay + limestone mixture, produced at temperatures of 1350 °C and 1450 °C**

| Cement | $D_{10}$ | $D_{50}$ | $D_{90}$ |
|---|---|---|---|
| CEM-AC0-1350 | 25.0 | 11.0 | 2.4 |
| CEM -AC49-1350 | 30.0 | 13.0 | 4.0 |
| CEM -AC74-1350 | 25.0 | 11.0 | 2.8 |
| CEM -AC0-1450 | 23.0 | 8.5 | 2.6 |
| CEM -AC49-1450 | 28.0 | 12.0 | 2.6 |
| CEM -AC74-1450 | 25.0 | 10.0 | 3.0 |

Table 7 shows the values of specific mass and specific surface areas (B.E.T. and Blaine) of the analyzed cements. It can be observed that the incorporation of ACW resulted in a reduction in the density of the cement since ACW has a lower specific mass compared to other raw materials such as limestone and clay. There was a decrease in the surface areas (Blaine and B.E.T.) of the cements when adding 49% and 74% ACW to the raw clinker mixture. Therefore, the reference cement (CIM-AC0) exhibited a smaller particle size, indicating that the grinding process was less efficient for the clinkers produced with ACW.

The physical properties of the cements containing ACW obtained in this study resemble those found by Schoon *et al.* (2012), who produced cements with 10% ACW incorporation and a Blaine surface area of 3,230 cm$^2$/g.

Cements with ACW showed lower loss on ignition, which is possibly associated with the partial substitution of limestone and the consequent reduction in the calcium carbonate content in the mixture. However, all cements demonstrated satisfactory loss on ignition (between 2.50% and 3.20%), as specified by NBR 16697 (ABNT, 2018).

## Hydration analysis of pastes

Figure 8 presents X-ray diffraction (XRD) analyses conducted on cement pastes produced with and without the addition of ACW at different stages (1, 3, 7, 28, and 91 days) to examine the hydration of the generated cements. The inclusion of ACW did not result in the formation of additional phases during the cement hydration process. According to this analysis, a reduction in the intensity of diffractometric peaks related to anhydrous phases can be observed from 1 to 91 days, particularly in the range between 32° and 33° (2Θ), mainly attributed to the alite and belite phases, respectively.

The pastes with cements produced with ACW did not show significant changes in the formation of the main ettringite peak when compared to the reference cement over time. It was also noted that the addition of ACW in the production of Portland clinker did not influence the formation of AFm phases, resulting from the conversion of ettringite, which occurs due to the low concentration of aluminates present in the cements as it is a poorly crystalline hydrate (Durdzinski *et al.*, 2015).

However, the incorporation of ACW in the production of Portland clinker intensified the formation of portlandite peaks in the first 24 hours due to the higher $C_3S$ content in the cement produced compared to the reference cement. In the early ages, the main reason for the small increase in the portlandite peaks is the higher C3S content in the cements produced with ACW compared to the reference cement. Studies by Zhou *et al.* (2018) reported that, after 1 day of hydration, cements produced with up to 1.50% $SO_3$ in the clinker meal show an increase in heat flow compared to cement without $SO_3$ addition. Yamashita et al. (2020), using up to 2.0% gypsum board waste in the clinker meal (3.40% $SO_3$), also observed an acceleration of the hydration process. In agreement Uda, Asakura and Nagashima (1998) reported that the addition of fly ash and slag to Portland clinker meals significantly affected the formation of alite and, consequently, the hydration of cementitious matrices at early ages.

Table 7 – **Specific mass, surface area (Blaine and B.E.T), and loss on ignition (LOI) of reference cements (CEM-AC0) and with the addition of 49% and 74% ACW in substitution for the clay + limestone mixture, produced at temperatures of 1350 °C and 1450 °C**

| Cement | Density (g/cm$^3$) | Especific surface area | *LOI |
|---|---|---|---|
| | | B.E.T (m$^2$/g) | |
| CEM-AC0-1350 | 3.78 ± 0.10 | 3.12 ± 0.07 | 3.14 ± 0.10 |
| CEM -AC49-1350 | 3.79 ± 0.30 | 2.78 ± 0.06 | 3.19 ± 0.12 |
| CEM -AC74-1350 | 3.63 ± 0.02 | 2.55 ± 0.09 | 2.50 ± 0.30 |
| CEM -AC0-1450 | 3.90 ± 0.15 | 4.60 ± 0.06 | 3.25 ± 0.01 |
| CEM -AC49-1450 | 3.71 ± 0.16 | 3.62 ± 0.08 | 3.04 ± 0.02 |
| CEM -AC74-1450 | 3.65 ± 0.24 | 3.25 ± 0.08 | 2.98 ± 0.12 |

**Note:** *loss on Igntion.

Figure 8 – **X-ray diffractograms of reference cement paste (without ACW) and with the addition of ACW, produced at temperatures of 1350 °C and 1450 °C after (A) 1 day, (B) 3 days, (C) 7 days, (D) 28 days, and (E) 91 days of hydration**

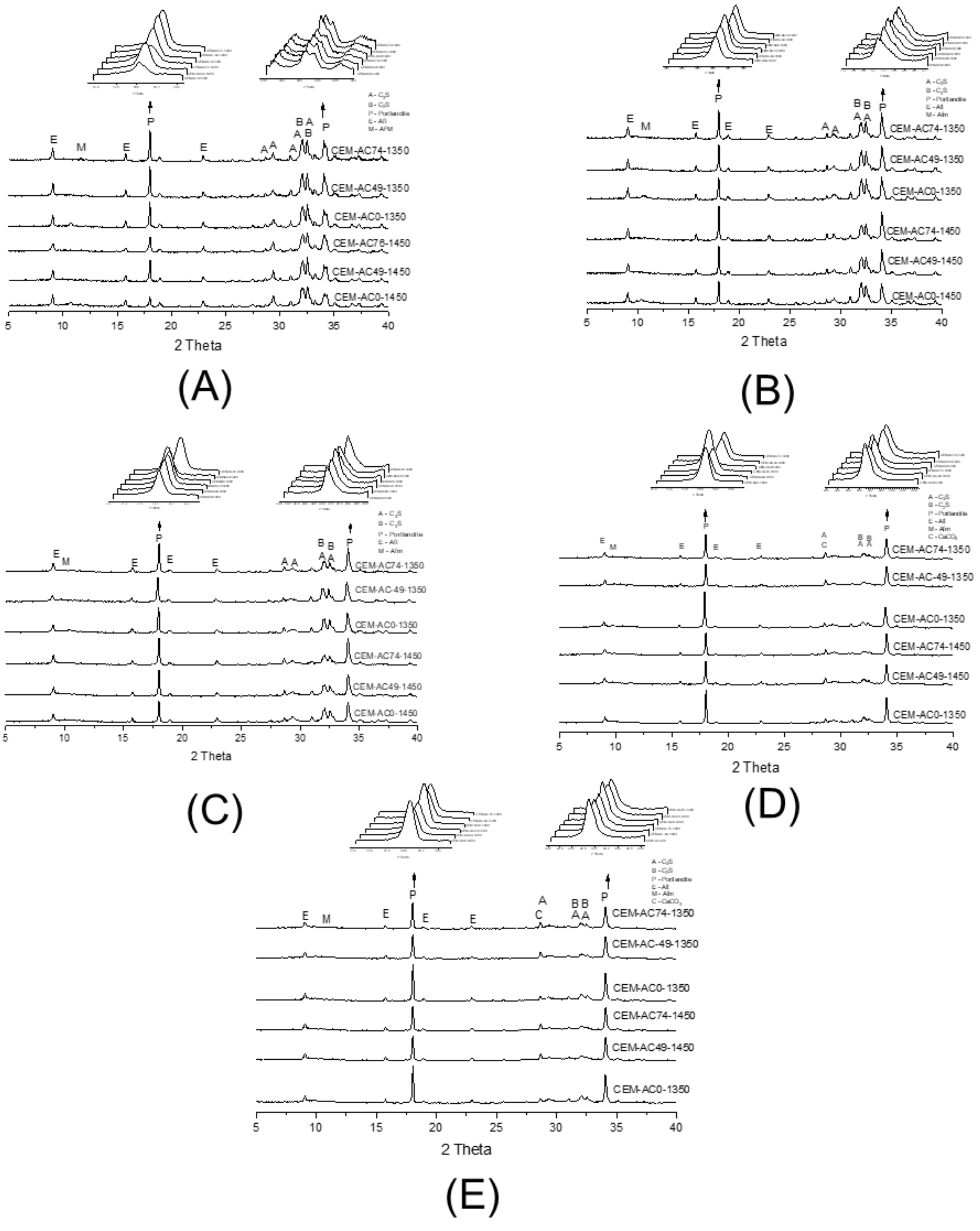

After the first 3 days of hydration, there was a minimal variation in the intensity of the portlandite peak in all produced cements. Finally, from the X-ray diffraction analysis, it was observed that the cements CEM-0, CEM 49, and CEM-AC74, produced at temperatures of 1350 °C and 1450 °C, exhibit similar levels of hydrated products at later ages, with no significant differences in the hydration kinetics. Yvon and Sharrock (2011) also observed that the addition of ACW in clinker production did not affect the hydration of cement matrices at later ages.

## Mechanical strength of cement pastes

For the analysis of axial compressive strength of the produced cement pastes, four cubic specimens (15 x 15 x 15 mm³) were used for each type of cement at each studied age (1, 3, 7, 28, and 91 days). The results are presented in Figure 9. Tables 8 and 9 present the ANOVA statistical evaluation regarding the mechanical strength of the produced cement pastes.

For pastes prepared with cements produced at 1350 °C and 1450 °C, an increase in axial compressive strength was observed in the early days of hydration for cements with ACW compared to reference cements. This increase can be attributed to the higher content of $C_3S$ available in cements with ACW, a behavior also identified by Odler and Zhang (1996), who added 1.80% of $SO_3$ to the clinker, resulting in accelerated axial compressive strength development. Additionally, no significant difference in compressive strength was observed between cements with 49% and 74% ACW.

At 28 days, the axial compressive strengths of all cements were similar, regardless of the presence or absence of ACW and the clinkering temperature. Stanek and Sulovsky (2002) and Taylor (1997) suggest that cements with higher levels of belite may exhibit a slower hydration rate, resulting in increased cement strength at later ages.

Studies conducted by Zhou *et al.* (2018) reported that cements with up to 1.50% of $SO_3$ in the clinker mixture showed a 13.0% increase in mechanical strength after 1 day of hydration compared to cement without $SO_3$ addition. However, after 28 days of curing, the increase was only 9.5%. Yamashita *et al.* (2020) also observed that compressive strength increased for clinkers with up to 1.2% of $SO_3$ after 3 days of hydration but decreased after 28 days.

Figure 9 – **Axial compressive strength at 1, 3, 7, 28, and 91 days of the pastes produced with reference cements (CEM-AC0) and with the addition of 49% and 74% ACW in substitution for the clay+limestone mixture, produced at temperatures of 1350 °C and 1450 °C**

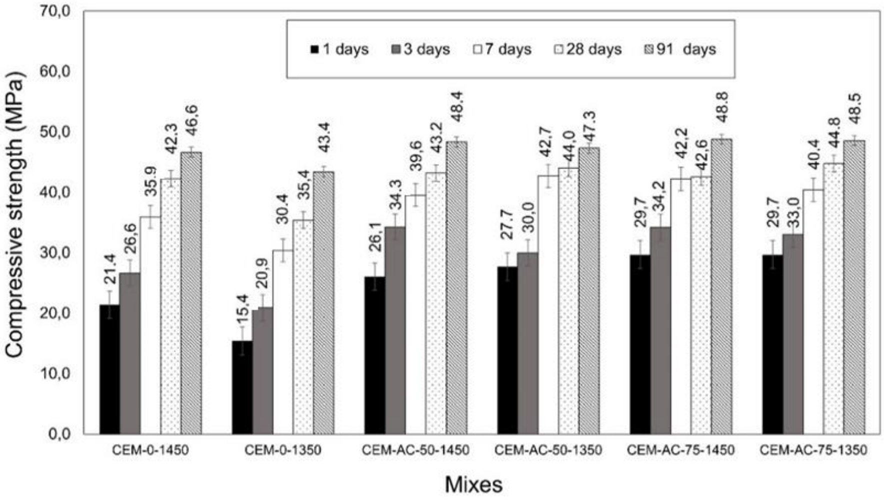

Table 8 – **Summary of the ANOVA statistical analysis of the mechanical strength of cement pastes produced with ACW at 1350 °C compared to the reference samples (without ACW)**

| Age | SQ | GL | MQ | F | P | Fc | Significant Effect |
|---|---|---|---|---|---|---|---|
| 1 day (AC-1350) | 415.49 | 2.00 | 207.74 | 32.09 | 0.00 | 4.26 | Yes |
| 3 days (AC-1350) | 358.43 | 2.00 | 179.21 | 35.52 | 0.00 | 4.26 | Yes |
| 7 days (AC-1350) | 283.67 | 2.00 | 141.84 | 9.85 | 0.01 | 4.74 | Yes |
| 28 days (AC-1350) | 143.98 | 2.00 | 71.99 | 5.76 | 0.03 | 4.46 | Yes |
| 91 days (AC-1350) | 11.78 | 2.00 | 5.89 | 0.32 | 0.73 | 4.26 | No |

Table 10 - **Summary of the ANOVA statistical analysis of the mechanical strength of cement pastes produced with ACW at 1450 °C compared to the reference samples (without ACW)**

| Age | SQ | GL | MQ | F | P | Fc | Significant Effect |
|---|---|---|---|---|---|---|---|
| 1 day (AC-1450) | 90.26 | 2.00 | 45.13 | 10.82 | 0.01 | 4.74 | Yes |
| 3 days (AC-1450) | 522.23 | 2.00 | 261.11 | 4.87 | 0.03 | 3.89 | Yes |
| 7 days (AC-1450) | 126.47 | 2.00 | 63.24 | 3.96 | 0.06 | 4.26 | No |
| 28 days (AC-1450) | 1.26 | 2.00 | 0.63 | 0.04 | 0.96 | 4.26 | No |
| 91 days (AC-1450) | 17.43 | 2.00 | 8.71 | 0.47 | 0.64 | 4.26 | No |

It is important to highlight that the compressive strength values of the cement pastes produced with ACW incorporation are comparable to those of commercial Portland cement pastes, meeting the strength requirements defined by the Brazilian standard NBR 16697 (ABNT, 2018). Finally, it is relevant to emphasize that the mechanical strength results are consistent with XRD analyses of the pastes, indicating that ACW accelerates the initial hydration reactions when added to Portland clinker mixtures.

### Expansibility

Table 10 presents the results of cold expansibility of the reference cements and those containing 49% and 74% ACW, produced at 1350 °C and 1450 °C, obtained from Le Chatelier needles.

The cements containing ACW and produced at 1350 °C showed a cold expansibility of 3.00 mm (CEM-49AC-1350) and 3.20 mm (CEM-74AC-1350), while those produced at 1450 °C exhibited an expansibility of 0.95 mm (CEM-49AC-1450) and 1.0 mm (CEM-49AC-1450), respectively. It was observed that there was an increase in the expansibility of the cements with ACW addition compared to the reference cements CEM-AC0-1350 and CEM-AC-1350. This increase in expansibility of the produced cements is likely related to the high content of periclase (up to 11.50%) present in the clinkers made with ACW. Although the incorporation of ACW in Portland clinkers led to an increase in the expansibility of the produced matrices, it was found that all cements met the recommendations of standard NBR 11582 (ABNT, 1991), presenting values lower than the permitted limit (5 mm).

## Conclusions

Based on the results obtained during the experimental program and the analyses conducted throughout the study, the following conclusions can be highlighted:

(a) different additions of ACW were analyzed, incorporated into the limestone and clay mixture. The results showed that there is chemical compatibility between ACW and the other raw materials constituting clinker, and its incorporation into the clinkerization process did not result in negative indicators for the main characteristics of Portland cement;

(b) ACW acts as a mineralizer, accelerating reactions in the clinkerization process and increasing the percentage of alite present in the clinker. The mixture containing 74% ACW incorporation produced at 1350 °C with 1.27% $SO_3$ resulted in a clinker with a higher alite content compared to the others;

(c) the addition of ACW (up to 1.69% $SO_3$) to the clinker led to a reduction in the $C_3A$ content in the cement;

(d) according to the mineralogical characterization of the pastes of cements with ACW, an increase in the quantity of hydrated products was observed only in the early ages; and

(e) the physical-mechanical performance of pastes made with cements produced with 74% and 49% ACW at 1350 °C, at 91 days, was similar to that of pastes made at 1450 °C, allowing their use in the production of cementitious matrices.

Table 9 – **Cold expansibility of reference cements (CIM-AC0) and with the addition of 49% and 74% ACW in replacement of the clay + limestone mixture, produced at temperatures of 1350 °C and 1450 °C**

| Cement | Expansibility |
|---|---|
| CEM-AC0-1350 | 1.20 ± 0.30 |
| CEM-AC49-1350 | 3.00 ± 0.10 |
| CEM-AC74-1350 | 3.20 ± 0.30 |
| CEM-AC0-1450 | 0.65 ± 0.23 |
| CEM-AC49-1450 | 0.95 ± 0.25 |
| CEM-AC74-1450 | 1.00 ± 0.20 |
| Normative Limit - NBR 11582 (ABNT, 1991) | < 5.00 |

Therefore, the use of ACW as a raw material in the production of Portland clinker is highly promising, allowing the utilization of a hazardous waste and increasing the reactivity of the mixture, resulting in an increase in alite content and, consequently, better mechanical performance of cements at early ages.

## References

AMERICAN SOCIETY FOR TESTING MATERIALS. **C150**: standard specification for portland cement. Philadelphia, 1997.

ANDRADE NETO, J. S. *et al*. Effects of $TiO_2$ waste on the formation of clinker phases and mechanical performance and hydration of Portand cement. **Cement**, v. 9, 100036, 2022.

ASSOCIAÇÃO BRASILEIRA DE NORMAS TÉCNICAS. **NBR 16697**: cimento Portland: requisitos. Rio de Janeiro, 2018.

ASSOCIAÇÃO BRASILEIRA DE NORMAS TÉCNICAS. **NBR 7215**: cimento Portland: determinação da resistência à compressão. Rio de Janeiro, 1996.

ASSOCIAÇÃO BRASILEIRA DE NORMASTÉCNICAS. **NBR 11582**: cimento Portland: determinação da expansibilidade de Le Chatelier. Rio de Janeiro, 1991.

BELARDI, G.; PIGA, L. Influence of calcium carbonate on the decomposition of asbestos contained in end-of-life products. **Thermochimica Acta**, v. 573, p. 220-228, 2013.

BOHÁČ, M. *et al*. The role of $Li_2O$, MgO and CuO on $SO_3$ activated clinkers. **Cement and Concrete Research**, v. 152, p. 106672–106672, 2022.

BRITISH STANDARD INSTITUTE. **BS EN 196-3:** methods of testing cement: determination of setting times and soundness (+A1:2008). London, 2005.

CAO, Z. *et al*. The sponge effect and carbon emission mitigation potentials of the global cement cycle**.** **Nature Communications**, v. 11, n. 1, jul. 2020.

CARNEIRO, G. O. *et al*. Thermal treatment optimization of asbestos cement waste (ACW) potentializing its use as alternative binder. **Journal of Cleaner Production**, v. 320, p. 128801, 2021.

CEMENT SUSTAINABILITY INITIATIVE. **Cement sustainability initiative**. Available: https://www.wbcsd.org/resources/technology-roadmap-low-carbon-transition-in-the-cement-industry/. Access: 23 mar. 2021.

CHATTERJEE, A. K. Chemistry and engineering of the clinkerization process: incremental advances and lack of breakthroughs. **Cement and Concrete Research**, v. 41, n. 7, p. 624–641, 2011.

COLVILLE, A. A.; GELLER, S. The crystal structure of brownmillerite, $Ca_2FeAlO_5$. **Acta Crystallographica Section B: Structural Crystallography and Crystal Chemistry**, v. 27, n. 12, p. 2311-2315, 1971.

COSTA, E. B. *et al*. Clínquer Portland com reduzido impacto ambiental. **Ambiente Construído,** Porto Alegre, v. 13, n. 2, p. 75-86, abr./jun. 2013.

DE LA TORRE, Á. G. *et al*. In situ synchrotron powder diffraction study of active belite clinkers. **Journal of Applied Crystallography**, v. 40, n. 6, p. 999-1007, 2007.

DURDZIŃSKI, P. T. *et al.* A new quantification method based on SEM-EDS to assess fly ash composition and study the reaction of its individual components in hydrating cement paste. **Cement and Concrete Research**, v. 73, p. 111-122, 2015.

FARIA, N. C. N. *et al.* Clinker Portland with iron ore tailing and its characterization by integrated laboratory methods. **Construction and Building Materials**, v. 402, p. 132958–132958, 2023.

FLANAGAN, D. M. Asbestos. **Science for a changing world**, p. 26–27, 2019.

GHAZI, A. B.; JAMSHIDI-ZANJANI, A.; NEJATI, H. Clinkerisation of copper tailings to replace Portland cement in concrete construction. **Journal of Building Engineering**, v. 51, p. 104275, 2022.

GOMES *et al.* Mineralogical Analysis of Portland Clinker Produced from the Incorporation of Granitic Rock Fines (GRF). **Key Engineering Materials**, v. 803, p. 309–313, 2019.

HE, X. *et al.* Multi-solid waste collaborative production of clinker-free cemented iron tailings backfill material with ultra-low binder-tailing ratio. **Construction and Building Materials**, v. 367, p. 130271–130271, 2023.

HER, S. *et al.* Feasibility study on utilization of pulverized eggshell waste as an alternative to limestone in raw materials for Portland cement clinker production. **Construction and Building Materials**, v. 324, p. 126589, 2022.

INTERGOVERNMENTAL PANEL ON CLIMATE CHANGE. **Climate change 2022**: mitigation of climate change, the working group III contribution to the Sixth Assessment Report. Available: https://www.unep.org/resources/report/climate-change-2022-mitigation-climate-change-working-group-iii-contribution-sixth. Access: 23 out. 2023.

INTERNATIONAL RESOURCE PANEL. **Global resources outlook**. Available: https://www.resourcepanel.org/reports/global-resources-outlook. Access: 15 fev. 2023.

IWASZKO, J.; ZAWADA, A.; LUBAS, M. Influence of high-energy milling on structure and microstructure of asbestos-cement materials. **Journal of Molecular Structure**, v. 1155, p. 51–57, 2018.

KATYAL, N. K. *et al.* Rapid estimation of free magnesia in OPC clinker and 3CaO: $1SiO_2$ system by complexometry. **Cement and concrete research**, v. 28, n. 4, p. 481-485, 1998.

KOLOVOS, K. *et al.* The effect of foreign ions on the reactivity of the $CaO–SiO_2–Al_2O_3–Fe_2O_3$ system: Part I. Anions. **Cement and Concrete Research**, v. 31, n. 3, p. 425-429, 2001.

MAKI, I. *et al.* Clinker grindability and textures of alite and belite. **Cement and Concrete Research**, v. 23, n. 5, p. 1078-1084, 1993.

MAKI, I.; GOTO, K. Factors influencing the phase constitution of alite in portland cement clinker. **Cement and Concrete Research**, v. 12, n. 3, p. 301–308, 1982.

MEHTA, P. K.; GJORV, O. E. A new test for sulfate resistance of cements. **Journal of Testing and Evaluation**, v. 2, p. 510-515, 1974.

MONDAL, P.; JEFFERY, J. W. The crystal structure of tricalcium aluminate, $Ca_3Al_2O_6$. **Acta Crystallographica Section B: Structural Crystallography and Crystal Chemistry**, v. 31, n. 3, p. 689-697, 1975.

ODLER, I.; ZHANG, H. Investigations on high $SO_3$ portland clinkers and cements I. Clinker synthesis and cement preparation. **Cement and concrete research**, v. 26, n. 9, p. 1307-1313, 1996.

PRIMAK, W.; KAUFMAN, H.; WARD, R. X-ray diffraction studies of systems involved in the preparation of alkaline earth sulfide and selenide phosphors1. **Journal of the American Chemical Society**, v. 70, n. 6, p. 2043-2046, 1948.

RAINA, K.; JANAKIRAMAN, L. K. Use of mineralizer in black meal process for improved clinkerization and conservation of energy. **Cement and Concrete Research**, v. 28, n. 8, p. 1093-1099, 1998.

RANAIVOMANANA, H.; LEKLOU, N. Investigation of microstructural and mechanical properties of partially hydrated Asbestos-Free fiber cement waste (AFFC) based concretes: experimental study and predictive modeling. **Construction and Building Materials**, v. 277, 121943, 2021.

SANTOS, T. A. *et al*. Influence of the content of alkalis ($Na_2O$ and $K_2O$), MgO, and $SO_3$ present in the granite rock fine in the production of Portland clinker. **Journal of Materials in Civil Engineering**, v. 34, n. 3, 2022.

SANTOS, T. A.; CILLA, M. S.; RIBEIRO, E. D. V. Use of asbestos cement tile waste (ACW) as mineralizer in the production of Portland cement with low $CO_2$ emission and lower energy consumption. **Journal of Cleaner Production**, v. 335, 130061, 2022.

SASAKI, S.; FUJINO, K.; TAKÉUCHI, Y. X-ray determination of electron-density distributions in oxides, MgO, MnO, CoO, and NiO, and atomic scattering factors of their constituent atoms. **Proceedings of the Japan Academy, Series B**, v. 55, n. 2, 1979.

SCHEPPER, M. *et al.* The regeneration of cement out of Completely Recyclable Concrete: Clinker production evaluation. **Construction and Building Materials**, v. 38, p. 1001–1009, 2013.

SCHOON, J. *et al*. Waste fibrecement: an interesting alternative raw material for a sustainable Portland clinker production. **Construction and Building Materials**, v. 36, p. 391–403, 2012.

SOHN, I. *et al.* Influence of TiO2 on the viscous behavior of calcium silicates melts containing 17 mass% Al2O3 and 10 mass% MgO. **ISIJ International**, v. 52, n. 1, p. 158-160, 2012.

SPASIANO, D.; PIROZZI, F. Treatments of asbestos containing wastes. **Journal of Environmental Management**, v. 204, p. 82-91, 2017.

STANĚK, T.; SULOVSKÝ, P. The influence of the alite polymorphism on the strength of the Portland cement. **Cement and Concrete Research**, v. 32, n. 7, p. 1169–1175, 2002.

STAYNER, L.; WELCH, L. S.; LEMEN, R. The worldwide pandemic of asbestos-related diseases. **Annual Review of Public Health**, v. 34, n. 1, p. 205–216, 2013.

TAYLOR, H. F. W. **Cement chemistry**. London: Telford, 1997.

UDA, S.; ASAKURA, E.; NAGASHIMA, M. Influence of $SO_3$ on the phase relationship in the system $CaO–SiO_2–Al_2O_3–Fe_2O_3$. **Journal of the American Ceramic Society**, v. 81, n. 3, p. 725-729, 1998.

VIANI, A. *et al.* Crystal chemistry of the high temperature product of transformation of cement-asbestos. **Journal of Hazardous Materials**, v. 248–249, n. 1, p. 69–80, 2013.

VIANI, A.; GUALTIERI, A. F. Preparation of magnesium phosphate cement by recycling the product of thermal transformation of asbestos containing wastes. **Cement and Concrete Research**, v. 58, p. 56–66, 2014.

VILAPLANA, A.S.G. *et al.* Utilization of Ladle Furnace slag from a steelwork for laboratory scale production of Portland cement. **Construction and Building Materials**, v. 94, p. 837–843, set. 2015.

WINTER, N. B. **Understanding cement**: the fast star user-friendly insight into cement production, cement hydration and cement and concrete chemistry. Woodbridge: WHD Microanalysis Consultants Lt, 2012.

WORLD BUSINESS COUNCIL FOR SUSTAINABLE DEVELOPMENT. **Cement sustainability iniative**: progress report. 2012. Available: http://www.wbcsd.org. Access: 20 dez. 2017.

YAMASHITA, M. *et al*. Influence of sulfur trioxide in clinker on the hydration heat and physical properties of Portland cement. **Construction and Building Materials**, v. 250, p. 118844, 2020.

YANG, Q. *et al*. Study on the composition and hydration properties at early stages of high-sodium Portland cement clinker under the synergistic effects of $SO_3$. **Construction and Building Materials**, v. 400, 132696, 2023.

YOUNG, G.; YANG, M. Preparation and characterization of Portland cement clinker from iron ore tailings. **Construction and Building Materials**, v. 197, p. 152–156, 2019.

YVON, Y.; SHARROCK, P. Characterization of thermochemical inactivation of asbestos containing wastes and recycling the mineral residues in cement products. **Waste and Biomass Valorization**, v. 2, p. 169-181, 2011.

ZHOU, H. *et al*. Research on the formation of $M_1$-type alite doped with MgO and $SO_3$: a route to improve the quality of cement clinker with a high content of MgO. **Construction and Building Materials**, v. 182, p. 156–166, 2018.

**Tiago Assunção Santos**
Conceptualization, Data curation, Formal analysis, Investigation, Methodology, Validation, Visualization, Writing – original draft.

Departamento de Tecnologia | Universidade Estadual de Feira de Santana | Av. Transnordestina, s/n, Novo Horizonte | Feira de Santana – BA – Brasil | CEP 44036-900 | Tel.: (75) 3161-8310 | E-mail: tiagoassuncao@hotmail.com

**Marcelo Strozi Cilla**
Writing – review & editing, Funding acquisition, Project administration, Resources, Supervision, Writing – original draft.

Departamento de Ciência dos Materiais | Universidade Federal da Bahia | Rua Prof. Aristides Novis, 02, Federação | Salvador – BA – Brasil | CEP 40210-630 | Tel.: (71) 3283–9852 | E-mail: marceloscilla@gmail.com

**Daniel Véras Ribeiro**
Writing – review & editing, Funding acquisition, Project administration, Resources, Supervision, Writing – original draft.

Departamento de Ciência dos Materiais | Universidade Federal da Bahia | E-mail: verasribeiro@hotmail.com

Editores: **Marcelo Henrique Farias de Medeiros** e **Eduardo Pereira**

***Ambiente Construído***
Revista da Associação Nacional de Tecnologia do Ambiente Construído
Av. Osvaldo Aranha, 99 - 3º andar, Centro
Porto Alegre – RS - Brasil
CEP 90035-190
Telefone: +55 (51) 3308-4084
www.seer.ufrgs.br/ambienteconstruido
www.scielo.br/ac
E-mail: ambienteconstruido@ufrgs.br